IEEE Access
Multidisciplinary ⋮ Rapid Review ⋮ Open Access Journal

Received September 16, 2020, accepted September 28, 2020, date of publication October 6, 2020, date of current version October 19, 2020.

Digital Object Identifier 10.1109/ACCESS.2020.3029066

Recurrent Neural Network Based Robust Actuator and Sensor Fault Estimation for Satellite Attitude Control System

DIZHI LONG[1], XIN WEN[1], WEI ZHANG[2], AND JUNHONG WANG[1]
[1]College of Astronautics, Nanjing University of Aeronautics and Astronautics, Nanjing 210016, China
[2]College of Information Engineering, Beijing Institute of Petrochemical Technology, Beijing 102617, China

Corresponding author: Wei Zhang (zhangwei_bipt@126.com)

This work was supported in part by the Foundation of Graduate Innovation Center in the Nanjing University of Aeronautics and Astronautics under Grant kfjj20181507, and in part by the Experimental Technology Research and Development Project 2019 of the Nanjing University of Aeronautics and Astronautics under Grant 2018051500052412.

ABSTRACT For the satellite attitude control system with actuator and sensor fault, the paper proposes a neural network based robust state and fault estimation method. Compared with the traditional model-based approach that relies on the accurate model of the system, we train the recurrent neural network with the inputs and outputs of the current attitude control system to achieve the purpose of modeling and improving the accuracy of the model. Then, through the expansion of the system state vectors, the neural state space model is transformed into a generalized nonlinear system without sensor fault terms. Furthermore, a combination of the generalized unknown input observer scheme with the robust $H\infty$ linear parameter-varying (LPV) approach is developed to estimate the system state and actuator faults simultaneously. According to Lyapunov theory, the stability analysis of observer is considered by transforming the dynamic error into the discrete time polytopic LPV form. Finally, some tests are performed on the satellite attitude control system to validate the effectiveness of the proposed method.

INDEX TERMS Fault estimation, recurrent neural network, satellite attitude control system, unknown input observer, Lyapunov theory.

I. INTRODUCTION

Satellite is a complex equipment which integrates technologies of different area including optics, electricity, mechanical and so on. Due to long-term working in the space environment of weightlessness, large temperature difference and strong radiation, its components are prone to fault. Among them, the fault rate of attitude control system (ACS) is higher than other satellite subsystems [1], [2]. As one of the most important subsystems of satellite, the fault of ACS will lead to the reduction of control accuracy and instability of closed-loop control. In severe cases, it will shorten the life of the satellite or even interrupt the space mission.

Since the 1990s, with the improvement of satellite complexity and reliability requirement, engineers have profoundly researched in nonlinear system fault detection and isolation (FDI) [3]–[5]. They have a common point of view that a fast detection of small abrupt or incipient faults can prevent the system more serious fault. For such a reason, numerous efforts were focused on developing efficient and robust fault detection methods and fruitful results can be found in the literatures. Wang *et al.* [6] achieved the dynamic event-triggered fault detection for a class of discrete-time systems by zonotopic residual evaluation. An integral-based event-triggered condition and fault detection filter coordinated design method was provided in [7]. A mixed $H-/H\infty$ fault detection observer design criterion was developed for LPV system in finite frequency domain in [8]. However, the problems of fault estimation and identification were marginalized.

The final goal of fault diagnosis is to ensure the system can operate effectively even if faults occurring [9]–[12]. In order to realize the fast and accurate fault-tolerant control (FTC) of satellite, it is necessary to obtain the fault value and change trend of ACS. Thus, it is of great practical significance to propose an effective fault estimation method.

The associate editor coordinating the review of this manuscript and approving it for publication was Zhongyang Fei.

This work is licensed under a Creative Commons Attribution 4.0 License. For more information, see https://creativecommons.org/licenses/by/4.0/

In the past ten years, many experts and scholars have done a series of research on the fault estimation of ACS of satellite and made some progress. Yi *et al.* [13] proposed an indirect approach for fault diagnosis and fault-tolerant control in the satellite ACS with sampled-data measurements. By considering the fault term as an auxiliary state vector, a state augmented observer was designed to estimate the system state and fault. Jia *et al.* [14] and Cheng *et al.* [15] addressed the problem of integrated fault reconstruction and fault-tolerant control in satellite ACS subject to actuator faults via an integrated design of the observer and the fault-tolerant controller. A data-driven explicit state space based fault detection, isolation and estimation filter was proposed and developed in [16]. The estimation errors can be effectively compensated by using the input-output measurements and the estimated system Markov parameters. Gao *et al.* [17] proposed an integrated robust fault diagnosis method of satellite ACS based on nonlinear adaptive unknown input observer (UIO). It can reconstruct the isolated actuator fault by adaptive technology. For sensors, a robust fault reconstruction method based on reduced order sliding mode observer was proposed and applied to the fault reconstruction of satellite gyro [18]. Zhang *et al.* [19] researched the problem of observer based sliding mode fault tolerant control of satellite. In the presence of space disturbance torque, a proportional learning observer (PLO) was designed to estimate the fault of satellite flywheel.

It should be noted that most of the satellite fault diagnosis methods in the literatures are for actuator fault, while the research on sensor fault is relatively less. Because from the perspective of the FTC, we usually focus on fault diagnosis of actuators in the control process. However, the ACS consists of plant, actuators and sensors. The occurrence of sensor fault will also affect the efficiency of FTC to a certain extent [20]. Moreover, it is generally assumed that the faults do not occur at the same time i.e. only one kind of fault occurs. Therefore, it is still valuable to study fault estimation for simultaneous faults.

At present, observer-based approaches, especially UIO, are particularly attractive in fault estimation. It follows from the fact that such a method allows reconstruction of the system state and unknown inputs on basis of the model and the measurements of the system inputs and outputs. In addition, UIO has characteristics of robustness because it is designed to reduce the influence of model uncertainty, thereby the reliability of fault diagnosis is improved [21], [22]. Unfortunately, the main disadvantage of UIO and other observer-based approaches follows from the fact that the analytical model of the diagnosed system is required, which is often impractical for satellites or deep space detectors.

In order to solve the above problems, the paper proposes a design method of UIO based on artificial neural network (ANN), which can realize the fault estimation of actuator and sensor simultaneously. The reason for the decision to use ANN is that they have some good properties, especially the modelling of complex nonlinear dynamic systems, parallel processing, as well as generalization and adaptively features [23]–[27]. However, the main weakness of the ANN is that it cannot guarantee the disturbances decoupling and convergence to the origin. Thus, the combination of the ANN modelling ability and LPV technique is introduced to design a robust fault detection and estimation scheme, so that the influence of disturbances is minimized in the $H\infty$ sense [28], [29]. Firstly, the recurrent neural network (RNN) is trained to represent the state space model of the current satellite by using the input and output signals of the satellite ACS in orbit. Then, for actuator and sensor faults in the system, the neural state space model is transformed into a generalized nonlinear system without sensor fault by extending the state vectors. Finally, the UIO which can estimate the system state and actuator fault simultaneously is designed for the RNN-based generalized system. In the design process of observer, the dynamic error is transformed into LPV form to prove the stability through Lyapunov. While guarantying observer convergence, a specified disturbance attenuation level is achieved with respect to the state and fault estimation errors. The contributions of this article include: 1) providing a novel observer synthesis procedure which is based on the concept of the UIO for the ACS actuator and sensor fault detection and estimation; 2) Overcoming the disadvantage of observer-based approaches that need analytical model through the RNN identifying system; and 3) Guaranteeing system convergence and robustness via combination of the RNN and LPV technique.

The paper is organized in the following parts. Section 2 presents RNN-based neural state space model and a method of the model transforming into a generalized nonlinear system. Section 3 describes the design procedure of the robust UIO using $H\infty$ framework for the actuator and sensor faults estimation. Section 4 shows a simulation example of the proposed approach in the actuator and sensor faults estimation of satellite ACS. Finally, Section 5 presents the conclusion.

II. RNN-BASED NEURAL STATE SPACE MODEL

The RNN provides a general identification model in the restricted sense that they can approximate uniformly any MIMO nonlinear dynamic system over a finite-time interval [30], [31]. The general class of discrete-time state space neural network considered in this work consists of three layers, as depicted in Fig. 1.

A discrete-time nonlinear neural state space model represented by proposed RNN is given as

$$\begin{aligned} \boldsymbol{x}^*(k+1) &= \boldsymbol{A}^*\boldsymbol{x}^*(k) + \boldsymbol{B}\boldsymbol{u}(k) + \boldsymbol{A}_0\boldsymbol{\sigma}(\boldsymbol{E}_0^*\boldsymbol{x}^*(k)) \\ \boldsymbol{y}(k) &= \boldsymbol{C}^*\boldsymbol{x}^*(k) \end{aligned} \tag{1}$$

where $\boldsymbol{x}^*(k) \in \mathbb{R}^n, \boldsymbol{y}(k) \in \mathbb{R}^p, \boldsymbol{u}(k) \in \mathbb{R}^m$ denote the system state, output and input, respectively. $\boldsymbol{C}^*$ is measurement matrix. $\boldsymbol{A}^*, \boldsymbol{A}_0, \boldsymbol{B}$ and $\boldsymbol{E}_0^*$ are real valued matrices of appropriate dimensions. They represent the weights which

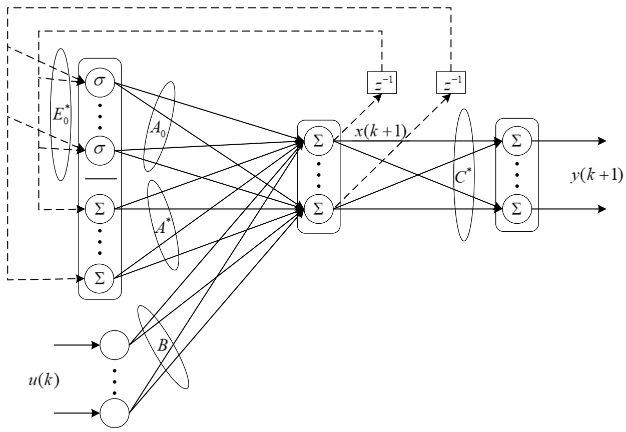

FIGURE 1. The structure of state space neural network.

will be adjusted during the training stage of RNN. The nonlinear activation function $\sigma(\cdot)$ is taken as a continuous, differentiable and bounded function.

Consider the following state space model that both contains actuator fault and sensor fault

$$\begin{aligned} \boldsymbol{x}^*(k+1) &= \boldsymbol{A}^*\boldsymbol{x}^*(k)+\boldsymbol{B}\boldsymbol{u}(k)+\boldsymbol{g}(\boldsymbol{x}^*(k))+\boldsymbol{D}\boldsymbol{f}_a(k)+\boldsymbol{W}\boldsymbol{\omega}(k) \\ \boldsymbol{y}(k) &= \boldsymbol{C}^*\boldsymbol{x}^*(k)+\boldsymbol{F}\boldsymbol{f}_s(k) \end{aligned} \tag{2}$$

where $\boldsymbol{g}(\boldsymbol{x}^*(k)) = A_0\sigma(\boldsymbol{E}_0^*\boldsymbol{x}^*(k)), \boldsymbol{f}_a(k) \in \mathbb{R}^q, \boldsymbol{f}_s(k) \in \mathbb{R}^s$ stand for the actuator fault and sensor fault, respectively. And $\boldsymbol{D}, \boldsymbol{F}$ are the matrices of appropriate dimensions. Without loss of generality, we assume $\boldsymbol{C}^*$ is row full rank and $\boldsymbol{D}, \boldsymbol{F}$ are column full rank. Moreover, $\boldsymbol{\omega}(k) \in l_2$ is an exogenous disturbance vector with $\boldsymbol{W} \in \mathbb{R}^{n\times m}$ being its distribution matrix while

$$l_2 = \left\{\boldsymbol{w} \in \mathbb{R}^m \mid \|\boldsymbol{w}\|_{l2} < \infty\right\}, \quad \|\boldsymbol{w}\|_{l2} = \left(\sum_{k=0}^{\infty} \|\boldsymbol{\omega}(k)\|_{l2}\right)^{1/2} \tag{3}$$

In order to estimate sensor fault, the following extended vectors are introduced.

$$\begin{aligned} \boldsymbol{x}(k) &= \begin{bmatrix}\boldsymbol{x}^*(k)^T & \boldsymbol{f}_s(k)^T\end{bmatrix}^T, \quad \boldsymbol{E} = \begin{bmatrix}\boldsymbol{I}_n & 0_{n\times s}\end{bmatrix}, \\ \boldsymbol{A} &= \begin{bmatrix}\boldsymbol{A}^* & 0_{n\times s}\end{bmatrix}, \quad \boldsymbol{E}_0 = \boldsymbol{E}_0^*\cdot\boldsymbol{E},\ \boldsymbol{C} = \begin{bmatrix}\boldsymbol{C}^* & \boldsymbol{F}\end{bmatrix}. \end{aligned}$$

It is obviously that $\boldsymbol{x}^*(k) = \boldsymbol{E}\boldsymbol{x}(k)$. In this way, the model (2) can be rewritten as:

$$\begin{aligned} \boldsymbol{E}\boldsymbol{x}(k+1) &= \boldsymbol{A}\boldsymbol{x}(k)+\boldsymbol{B}\boldsymbol{u}(k)+\boldsymbol{h}(\boldsymbol{x}(k))+\boldsymbol{D}\boldsymbol{f}_a(k)+\boldsymbol{W}\boldsymbol{\omega}(k) \\ \boldsymbol{y}(k) &= \boldsymbol{C}\boldsymbol{x}(k) \end{aligned} \tag{4}$$

where $\boldsymbol{h}(\boldsymbol{x}(k)) = A_0\boldsymbol{\sigma}(\boldsymbol{E}_0\boldsymbol{x}(k))$. Note that $\boldsymbol{F}$ is column full rank, we have $rank\begin{bmatrix}\boldsymbol{E}^T & \boldsymbol{C}^T\end{bmatrix}^T = n+s$ i.e. matrix $\begin{bmatrix}\boldsymbol{E}^T & \boldsymbol{C}^T\end{bmatrix}^T$ is column full rank. Therefore, there is a row full rank matrix $\begin{bmatrix}\boldsymbol{T} & \boldsymbol{N}\end{bmatrix} \in \mathbb{R}^{(n+s)\times(n+p)}$ such that $\begin{bmatrix}\boldsymbol{T} & \boldsymbol{N}\end{bmatrix}\begin{bmatrix}\boldsymbol{E}^T & \boldsymbol{C}^T\end{bmatrix}^T = \boldsymbol{I}_{n+s}$, namely

$$\boldsymbol{TE}+\boldsymbol{NC} = \boldsymbol{I}_{n+s} \tag{5}$$

The model (4) can be further written as:

$$\begin{aligned} \boldsymbol{x}(k+1) &= \boldsymbol{TAx}(k)+\boldsymbol{Ny}(k+1)+\boldsymbol{TBu}(k)+\boldsymbol{Th}(\boldsymbol{x}(k)) \\ &\quad +\boldsymbol{TDf}_a(k)+\boldsymbol{TW\omega}(k) \\ \boldsymbol{y}(k) &= \boldsymbol{Cx}(k) \end{aligned} \tag{6}$$

After the above processing, the original model (2) is transformed into the model (6) without sensor fault term. Hence, an observer is designed for model (6) to estimate system state and actuator fault simultaneously, which can estimate the state, sensor fault and actuator fault of satellite ACS.

III. UIO DESIGN FOR FAULTS ESTIMATION

The main purpose of this section is to provide a detailed design procedure of the robust UIO that can be used to detect and estimate actuator fault and sensor fault. In other words, the main function of the observer is to provide information about actuator fault and sensor fault.

Firstly, assuming the system is observable and the following rank condition is satisfied:

$$rank(\boldsymbol{CTD}) = rank(\boldsymbol{D}) = q \tag{7}$$

Substituting (6) into $\boldsymbol{y}(k+1) = \boldsymbol{Cx}(k+1)$, it can be shown that:

$$\begin{aligned} \boldsymbol{f}_a(k) = \boldsymbol{H}\big[&(\boldsymbol{I}_p-\boldsymbol{CN})\boldsymbol{y}(k+1)-\boldsymbol{CTAx}(k)-\boldsymbol{CTBu}(k) \\ &-\boldsymbol{CTh}(\boldsymbol{x}(k))-\boldsymbol{CTW\omega}(k)\big] \end{aligned} \tag{8}$$

Under the assumption (7), matrix $\boldsymbol{H}$ is possible calculated by

$$\boldsymbol{H} = (\boldsymbol{CTD})^+ = \left[(\boldsymbol{CTD})^T\boldsymbol{CTD}\right]^{-1}(\boldsymbol{CTD})^T \tag{9}$$

Finally, by substituting (8) into (6), it can be shown that:

$$\boldsymbol{x}(k+1) = \bar{\boldsymbol{A}}\boldsymbol{x}(k)+\bar{\boldsymbol{B}}\boldsymbol{u}(k)+\boldsymbol{Gh}(\boldsymbol{x}(k))+\bar{\boldsymbol{L}}\boldsymbol{y}(k+1)+\bar{\boldsymbol{W}}\boldsymbol{\omega}(k) \tag{10}$$

where, $\bar{\boldsymbol{A}} = \boldsymbol{GA}, \bar{\boldsymbol{B}} = \boldsymbol{GB}, \bar{\boldsymbol{L}} = (\boldsymbol{N}-\boldsymbol{TDHCN}+\boldsymbol{TDH}), \bar{\boldsymbol{W}} = \boldsymbol{GW}, \boldsymbol{G} = (\boldsymbol{T}-\boldsymbol{TDHCT})$. In order to estimate the state $\hat{\boldsymbol{x}}(k)$ and fault $\hat{\boldsymbol{f}}_a(k)$ of the system, the unknown input observer structure is designed as follows:

$$\begin{aligned} \hat{\boldsymbol{x}}(k+1) &= \bar{\boldsymbol{A}}\hat{\boldsymbol{x}}(k)+\bar{\boldsymbol{B}}\boldsymbol{u}(k)+\boldsymbol{Gh}(\hat{\boldsymbol{x}}(k)) \\ &\quad +\bar{\boldsymbol{L}}\boldsymbol{y}(k+1)+\boldsymbol{k}_a(\boldsymbol{y}(k)-\boldsymbol{C}\hat{\boldsymbol{x}}(k)) \end{aligned} \tag{11}$$

Consequently, the estimation of actuator fault is

$$\begin{aligned} \hat{\boldsymbol{f}}_a(k) = \boldsymbol{H}\big[&(\boldsymbol{I}_p-\boldsymbol{CN})\boldsymbol{y}(k+1)-\boldsymbol{CTA}\hat{\boldsymbol{x}}(k) \\ &-\boldsymbol{CTBu}(k)-\boldsymbol{CTh}(\hat{\boldsymbol{x}}(k))\big] \end{aligned} \tag{12}$$

Note that the proposed observer can be presented in the form of a neural network that is given in Fig. 2.

According to (11), the state estimation dynamic error is given by

$$\boldsymbol{e}(k+1) = \boldsymbol{x}(k+1)-\hat{\boldsymbol{x}}(k+1) = \boldsymbol{A}_1\boldsymbol{e}(k)+\bar{\boldsymbol{G}}\boldsymbol{s}(k)+\bar{\boldsymbol{W}}\boldsymbol{\omega}(k) \tag{13}$$

where $\boldsymbol{A}_1 = \bar{\boldsymbol{A}}-\boldsymbol{k}_a\boldsymbol{C}, \boldsymbol{s}(k) = \boldsymbol{h}(\boldsymbol{x}(k))-\boldsymbol{h}(\hat{\boldsymbol{x}}(k)), \bar{\boldsymbol{W}} = \boldsymbol{GW}$.

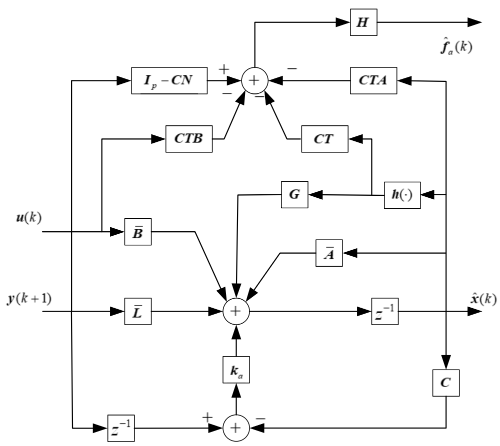

FIGURE 2. Neural network-based observer.

Similarly, the fault estimation dynamic error $\boldsymbol{e_f}(k)$ can be defined as

$$\boldsymbol{e_f}(k) = \boldsymbol{f}_a(k) - \hat{\boldsymbol{f}}_a(k) = -\boldsymbol{HCT}(\boldsymbol{Ae}(k) + \boldsymbol{s}(k) + \boldsymbol{W\omega}(k)) \tag{14}$$

Note that both $\boldsymbol{e}(k+1)$ and $\boldsymbol{e_f}(k)$ are nonlinear with respect to $\boldsymbol{e}(k)$. In order to transform them into LPV form, this article proposes the following solutions.

First, it is assumed that vector α depends on vector of measurable signal $\boldsymbol{\rho} \in \mathbb{R}^l$ referred to scheduling signal, according to

$$\boldsymbol{\alpha} = \boldsymbol{\kappa}(\boldsymbol{\rho}) \tag{15}$$

where $\boldsymbol{\kappa} : \mathbb{R}^s \to \mathbb{R}^r$ is continuous mapping. Let us define a convex polytope as a convex hull of a finite number of matrices $\boldsymbol{N}_i$

$$Co\{\boldsymbol{N}_i, i = 1, \ldots, r\} \triangleq \left\{ \sum_{i=1}^{r} \alpha_i \boldsymbol{N}_i, \sum_{i=1}^{r} \alpha_i = 1, \alpha_i \geq 0 \right\} \tag{16}$$

The time varying parameter $\boldsymbol{\alpha}$ varies in a polytope Θ, which is assumed to be a set of vertices $v_1, \ldots v_r$ that is

$$\boldsymbol{\alpha} \in \Theta = Co\{v_1, \ldots, v_r\} \tag{17}$$

Therefore, we can convert dynamic error (13) and (14) into polytopic LPV form. Now, define the following time varying parameter:

$$\boldsymbol{\alpha}_i = \begin{cases} \dfrac{\sigma(\boldsymbol{E}_0^{*i}\boldsymbol{x}^*(k))}{\boldsymbol{E}_0^{*i}\boldsymbol{x}^*(k)} & \boldsymbol{E}_0^{*i}\boldsymbol{x}^*(k) \neq 0 \\ 1 & \boldsymbol{E}_0^{*i}\boldsymbol{x}^*(k) = 0 \end{cases} \tag{18}$$

where $1 \leq i \leq r$ denotes *ith* row of a respective matrix. Then (2) can be written as:

$$\boldsymbol{x}^*(k+1) = \boldsymbol{A}^*\boldsymbol{x}^*(k) + \boldsymbol{Bu}(k) + \boldsymbol{A}_0\Theta_d\boldsymbol{E}_0^*\boldsymbol{x}^*(k) \tag{19}$$

with $\Theta_d \in \mathbb{R}^{r\times r}$ is a diagonal matrix that contains the variable parameters of the LPV model:

$$\Theta_d = \begin{bmatrix} \alpha_1 & 0 & \cdots & 0 \\ 0 & \alpha_2 & \cdots & 0 \\ \vdots & \vdots & \ddots & \vdots \\ 0 & 0 & \cdots & \alpha_r \end{bmatrix} \tag{20}$$

According to the above derivation, we can get

$$\boldsymbol{h}(\boldsymbol{x}(k)) = \sum_{i=1}^{r} \alpha_i \boldsymbol{A}_0^i \boldsymbol{E}_0^i \boldsymbol{x}(k) \tag{21}$$

Then the state estimation dynamic error (13) can be transformed into the following equation:

$$\boldsymbol{e}(k+1) = (\tilde{\boldsymbol{A}}(\alpha) - \boldsymbol{k}_a C)\boldsymbol{e}(k) + \bar{\boldsymbol{W}}\boldsymbol{\omega}(k) = \boldsymbol{A}_2(\boldsymbol{\alpha})\boldsymbol{e}(k) + \bar{\boldsymbol{W}}\boldsymbol{\omega}(k) \tag{22}$$

where

$$\tilde{\boldsymbol{A}}(\boldsymbol{\alpha}) = \boldsymbol{G}(\boldsymbol{A} + \sum_{i=1}^{r} \boldsymbol{\alpha}_i \boldsymbol{A}_0^i \boldsymbol{E}_0^i) \tag{23}$$

Similarly, the actuator fault estimation dynamic error (14) can be rewritten as

$$\begin{aligned} \boldsymbol{e_f}(k) &= -\boldsymbol{HCT}(\boldsymbol{A}_3(\boldsymbol{\alpha})\boldsymbol{e}(k) + \boldsymbol{W\omega}(k)) \\ \boldsymbol{A}_3(\boldsymbol{\alpha}) &= \boldsymbol{A} + \sum_{i=1}^{r} \boldsymbol{\alpha}_i \boldsymbol{A}_0^i \boldsymbol{E}_0^i \end{aligned} \tag{24}$$

The objective of further discussion is to design the observer (11) and (12) in such a way that the state estimation dynamic error $\boldsymbol{e}(k)$ is asymptotically convergent and the following upper bound is guaranteed:

$$\left\| \boldsymbol{e_f}(k) \right\|_{l2} \leq \varepsilon \left\| \boldsymbol{w} \right\|_{l2} \tag{25}$$

where $\varepsilon > 0$ is a prescribed disturbance attenuation level. On the contrary to the method proposed in the existing literatures, ε should be achieved with respect to the fault estimation error rather than the state estimation error.

Lemma 1: The following statements are equivalent:

(1) There exists $\boldsymbol{X} > 0$ such that

$$\boldsymbol{V}^T X V - \boldsymbol{W} < 0 \tag{26}$$

(2) There exists $\boldsymbol{X} > 0$ such that

$$\begin{bmatrix} -\boldsymbol{W} & \boldsymbol{V}^T\boldsymbol{U}^T \\ \boldsymbol{UV} & \boldsymbol{X} - \boldsymbol{U} - \boldsymbol{U}^T \end{bmatrix} < 0 \tag{27}$$

The subsequent theorem summarizes the main result of this section:

Theorem 1: For a prescribed disturbance attenuation level $\mu > 0$ for the fault estimation error, the $H\infty$ observer (11), (12) design problem for the model (6) is solvable if there exist matrices $\boldsymbol{P} > \boldsymbol{0}$, $\boldsymbol{U}$ and $\bar{\boldsymbol{N}}$ such that the following constraints are satisfied:

$$\begin{bmatrix} \boldsymbol{A}_3^T(\boldsymbol{\alpha})\boldsymbol{H}_1\boldsymbol{A}_3(\boldsymbol{\alpha}) - \boldsymbol{P} & \boldsymbol{A}_3^T(\boldsymbol{\alpha})\boldsymbol{H}_1\boldsymbol{W} & \boldsymbol{A}_2^T(\boldsymbol{\alpha})\boldsymbol{U}^T \\ \boldsymbol{W}^T\boldsymbol{H}_1\boldsymbol{A}_3(\boldsymbol{\alpha}) & \boldsymbol{W}^T\boldsymbol{H}_1\boldsymbol{W} - \mu^2\boldsymbol{I} & \bar{\boldsymbol{W}}^T\boldsymbol{U}^T \\ \boldsymbol{UA}_2(\boldsymbol{\alpha}) & \boldsymbol{U}\bar{\boldsymbol{W}} & \boldsymbol{P} - \boldsymbol{U} - \boldsymbol{U}^T \end{bmatrix} < 0 \tag{28}$$

with

$$\boldsymbol{k}_a = \boldsymbol{U}^{-1}\bar{\boldsymbol{N}} \tag{29}$$

$$\boldsymbol{U}\boldsymbol{A}_2(\boldsymbol{\alpha}) = \boldsymbol{U}\tilde{\boldsymbol{A}}(\boldsymbol{\alpha}) - \bar{\boldsymbol{N}}\boldsymbol{C} \tag{30}$$

where $\boldsymbol{H}_1 = \boldsymbol{T}^T\boldsymbol{C}^T\boldsymbol{H}^T\boldsymbol{H}\boldsymbol{C}\boldsymbol{T}$.

Proof: The problem of robust UIO observer design is to determine the gain matrix $\boldsymbol{k}_a$ such that

$$\lim_{k\to\infty} \boldsymbol{e}(k) = 0 \quad for\ \boldsymbol{\omega}(k) = \boldsymbol{0} \tag{31}$$

$$\left\|\boldsymbol{e}_f(k)\right\|_{l2} \le \varepsilon \left\|\boldsymbol{\omega}\right\|_{l2} \quad for\ \boldsymbol{\omega}(k) \ne \boldsymbol{0},\ \boldsymbol{e}_0 = \boldsymbol{0} \tag{32}$$

In this article, it is sufficient to find a Lyapunov function $V(k)$ for $k = 0, \ldots, \infty$ such that

$$\Delta V(k) + \boldsymbol{e}_f^T(k)\boldsymbol{e}_f(k) - \mu^2\boldsymbol{\omega}^T(k)\boldsymbol{\omega}(k) < 0 \tag{33}$$

where $\Delta V(k) = V(k+1) - V(k)$, $\mu > 0$. On one hand, if $\boldsymbol{\omega}(k) = \boldsymbol{0}$, then (33) boils down to

$$\Delta V(k) + \boldsymbol{e}_f^T(k)\boldsymbol{e}_f(k) < 0 \tag{34}$$

Hence $\Delta V(k) < 0$, which lead to (31). On the other hand, if $\boldsymbol{\omega}(k) \ne \boldsymbol{0}$, then (33) yields

$$J = \sum_{k=1}^{\infty}(\Delta V(k) + \boldsymbol{e}_f^T(k)\boldsymbol{e}_f(k) - \mu^2\boldsymbol{\omega}^T(k)\boldsymbol{\omega}(k)) < 0 \tag{35}$$

which can be written as

$$J = -V(0) + \sum_{k=1}^{\infty}\boldsymbol{e}_f^T(k)\boldsymbol{e}_f(k)) - \mu^2\sum_{k=1}^{\infty}\boldsymbol{\omega}^T(k)\boldsymbol{\omega}(k) \tag{36}$$

Knowing that $V(0) = 0$ for $\boldsymbol{e}(0) = \boldsymbol{0}$, (36) leads to (32) with $\varepsilon = \mu$. Since the general idea of designing the robust observer is given, the following Lyapunov function is given:

$$V(k) = \boldsymbol{e}^T(k)\boldsymbol{P}\boldsymbol{e}(k), \quad \boldsymbol{P} > 0 \tag{37}$$

As a consequence:

$$\begin{aligned}
&\Delta V(k) + \boldsymbol{e}_f^T(k)\boldsymbol{e}_f(k) - \mu^2\boldsymbol{\omega}^T(k)\boldsymbol{\omega}(k)\\
&\quad = \boldsymbol{e}^T(k)\left[\boldsymbol{A}_2^T(\boldsymbol{\alpha})\boldsymbol{P}\boldsymbol{A}_2(\boldsymbol{\alpha}) + \boldsymbol{A}_3^T(\boldsymbol{\alpha})\boldsymbol{H}_1\boldsymbol{A}_3(\boldsymbol{\alpha}) - \boldsymbol{P}\right]\boldsymbol{e}(k)\\
&\qquad + \boldsymbol{e}^T(k)\left[\boldsymbol{A}_2^T(\boldsymbol{\alpha})\boldsymbol{P}\bar{\boldsymbol{W}} + \boldsymbol{A}_3^T(\boldsymbol{\alpha})\boldsymbol{H}_1\boldsymbol{W}\right]\boldsymbol{\omega}(k)\\
&\qquad + \boldsymbol{\omega}^T(k)\left[\bar{\boldsymbol{W}}^T\boldsymbol{P}\bar{\boldsymbol{W}} + \boldsymbol{W}^T\boldsymbol{H}_1\boldsymbol{W} - \mu^2\boldsymbol{I}\right]\boldsymbol{\omega}(k)\\
&\qquad + \boldsymbol{\omega}^T(k)\left[\bar{\boldsymbol{W}}^T\boldsymbol{P}\boldsymbol{A}_2(\boldsymbol{\alpha}) + \boldsymbol{W}^T\boldsymbol{H}_1\boldsymbol{A}_3(\boldsymbol{\alpha})\right]\boldsymbol{e}(k) < 0
\end{aligned} \tag{38}$$

By defining

$$\varepsilon(k) = \begin{bmatrix}\boldsymbol{e}^T(k) & \boldsymbol{\omega}^T(k)\end{bmatrix}^T \tag{39}$$

(38) can be equivalent to

$$\Delta V(k) + \boldsymbol{e}_f^T(k)\boldsymbol{e}_f(k) - \mu^2\boldsymbol{\omega}^T(k)\boldsymbol{\omega}(k) = \varepsilon^T(k)\boldsymbol{\Xi}\varepsilon(k) < 0 \tag{40}$$

where Ξ is given by the equation (41), as shown at the bottom of the next page.

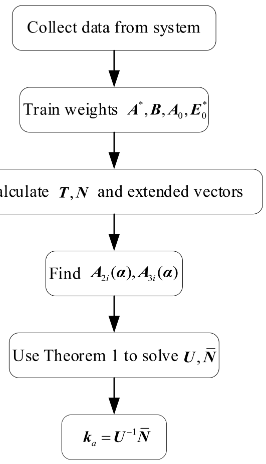

FIGURE 3. Block diagram of observer design procedure.

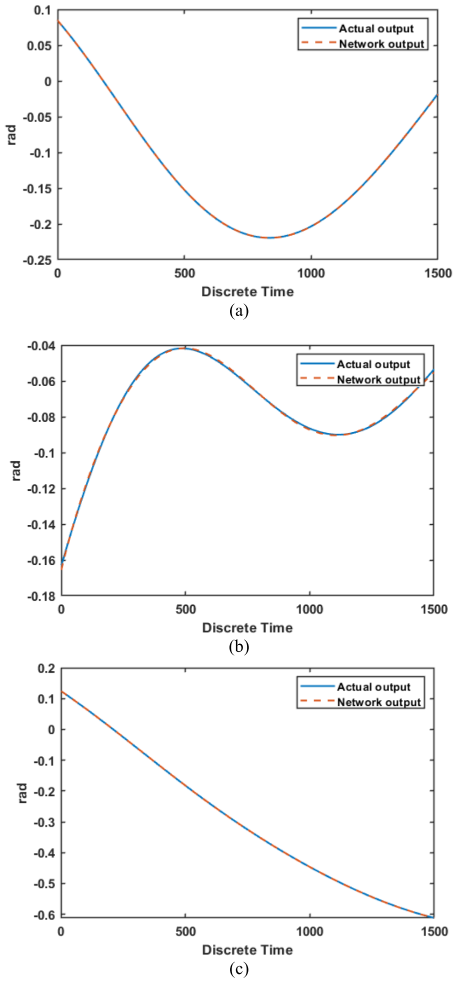

FIGURE 4. (a) Actual output and network output for φ; (b) Actual output and network output for θ; (c) Actual output and network output for ψ.

Furthermore, the matrix (41) can be written as:

$$\begin{bmatrix}\boldsymbol{A}_2^T(\boldsymbol{\alpha})\\ \bar{\boldsymbol{W}}^T\end{bmatrix}\boldsymbol{P}\begin{bmatrix}\boldsymbol{A}_2(\boldsymbol{\alpha}) & \bar{\boldsymbol{W}}\end{bmatrix} + \begin{bmatrix}\boldsymbol{A}_3^T(\boldsymbol{\alpha})\boldsymbol{H}_1\boldsymbol{A}_3(\boldsymbol{\alpha}) - \boldsymbol{P} & \boldsymbol{A}_3^T(\boldsymbol{\alpha})\boldsymbol{H}_1\boldsymbol{W}\\ \boldsymbol{W}^T\boldsymbol{H}_1\boldsymbol{A}_3(\boldsymbol{\alpha}) & \boldsymbol{W}^T\boldsymbol{H}_1\boldsymbol{W} - \mu^2\boldsymbol{I}\end{bmatrix} \tag{42}$$

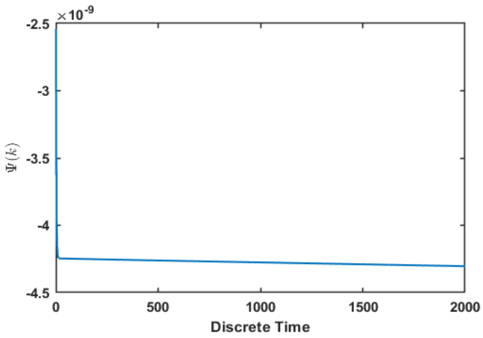

FIGURE 5. Evolution of $\Psi(k)$.

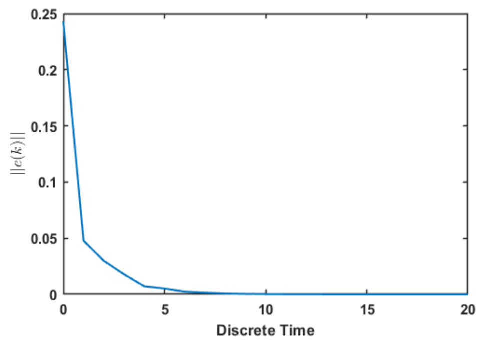

FIGURE 6. Evolution of $\|e(k)\|$.

According to Lemma 1, relation (40) is equivalent to

$$\begin{bmatrix} A_3^T(\alpha)H_1A_3(\alpha)-P & A_3^T(\alpha)H_1W & A_2^T(\alpha)U^T \\ W^TH_1A_3(\alpha) & W^TH_1W-\mu^2I & \bar{W}^TU^T \\ UA_2(\alpha) & U\bar{W} & P-U-U^T \end{bmatrix}<0 \tag{43}$$

which completes the proof.

Obviously, $A+\sum_{i=1}^{r}\alpha_iA_0^iE_0^i$ can be expressed as the convex sum of matrices. Therefore, the problem comes down to solving a set of LMIs

$$\begin{bmatrix} A_{3i}^T(\alpha)H_1A_{3i}(\alpha)-P & A_{3i}^T(\alpha)H_1W & A_{2i}^T(\alpha)U^T \\ W^TH_1A_{3i}(\alpha) & W^TH_1W-\mu^2I & \bar{W}^TU^T \\ UA_{2i}(\alpha) & U\bar{W} & P-U-U^T \end{bmatrix}<0, \quad i=1,\cdots,r \tag{44}$$

Finally, the observer design problem can be reduced to the following minimization task

$$\mu^*=\min_{\mu>0,P>0,U,\bar{N}}\mu \tag{45}$$

The design procedure of the actuator and sensor fault observer is summarized as shown in the Fig. 3.

IV. FAULT DIAGNOSIS OF THE SATELLITE ACS

In order to make a further explanation of above design procedure and verify the effectiveness of the proposed observer, we perform a simulation on the satellite ACS. A typical three-axis stable satellite is given by [32]–[34], the satellite orbit angular velocity $w_0=0.0012rad/s$ and the moment of inertial matrix $J_m = diag\{18.73, 20.77, 23.63\}\, kg\cdot m^2$. Considering the scene of small angle change of satellite attitude, the attitude angle $\begin{bmatrix}\varphi & \theta & \psi\end{bmatrix}^T$ and angular velocity $\begin{bmatrix}\dot\varphi & \dot\theta & \dot\psi\end{bmatrix}^T$ are selected as system state variables. The simulation model is built in MATLAB/Simulink, and the disturbance matrix is assumed as

$$W=\begin{bmatrix} 0 & 0 & 0 \\ 0 & 0 & 0 \\ 0 & 0 & 0 \\ 0.5 & 0 & 0 \\ 0 & 0.5 & 0 \\ 0 & 0 & 0.5 \end{bmatrix}.$$

At the beginning of the development, the neural state space model of the satellite ACS has to be obtained according to the proposed methodology. The RNN inputs are the input flow to the satellite system and the outputs are attitude angles φ, θ, ψ. Training data are acquired from the open loop control system simulated by sine function with the sampling time $T_p = 0.01s$. Each set consists of 1500 samples. In this way, training data can represent plant dynamics pretty well.

Training of the neural state space model is carried out off-line for the maximum of 200 iterations using Levenberg–Marquardt algorithm while the actual process stopping after 70 iterations. It is clear that the satellite attitude angles need to be measurable for the process of network training and the matrix C^* is not the part of the proposed RNN, so C^* needn't to be updated. At the same time, above constraint C^* is a row full rank matrix. It is reasonably assumed that C^* is a fixed-value matrix $C^*=\begin{bmatrix}I_p & 0_{p\times(n-p)}\end{bmatrix}$. The model (1) is able to fit the nonlinear behavior of the system by a proper selection of the model structure (the number of nonlinear units represented by the number of row r of E_0^*). We consider the numbers of neurons in nonlinear layer varying from 3 to 8 and carry out experimental training. Through the trials, the optimal structure is found with $r=4$ showing the best performance in simulations. As a result of a training process, the following matrices of the neural state space model were obtained A^*, B, A_0 and E_0^*, as shown at the bottom of the 8th page.

Fig. 4 shows the actual outputs of the satellite attitude system and the estimation outputs from the neural network

$$\Xi=\begin{bmatrix} A_2^T(\alpha)PA_2(\alpha)+A_3^T(\alpha)H_1A_3(\alpha)-P & A_2^T(\alpha)P\bar{W}+A_3^T(\alpha)H_1W \\ \bar{W}^TPA_2(\alpha)+W^TH_1A_3(\alpha) & \bar{W}^TP\bar{W}+W^TH_1W-\mu^2I \end{bmatrix} \tag{41}$$

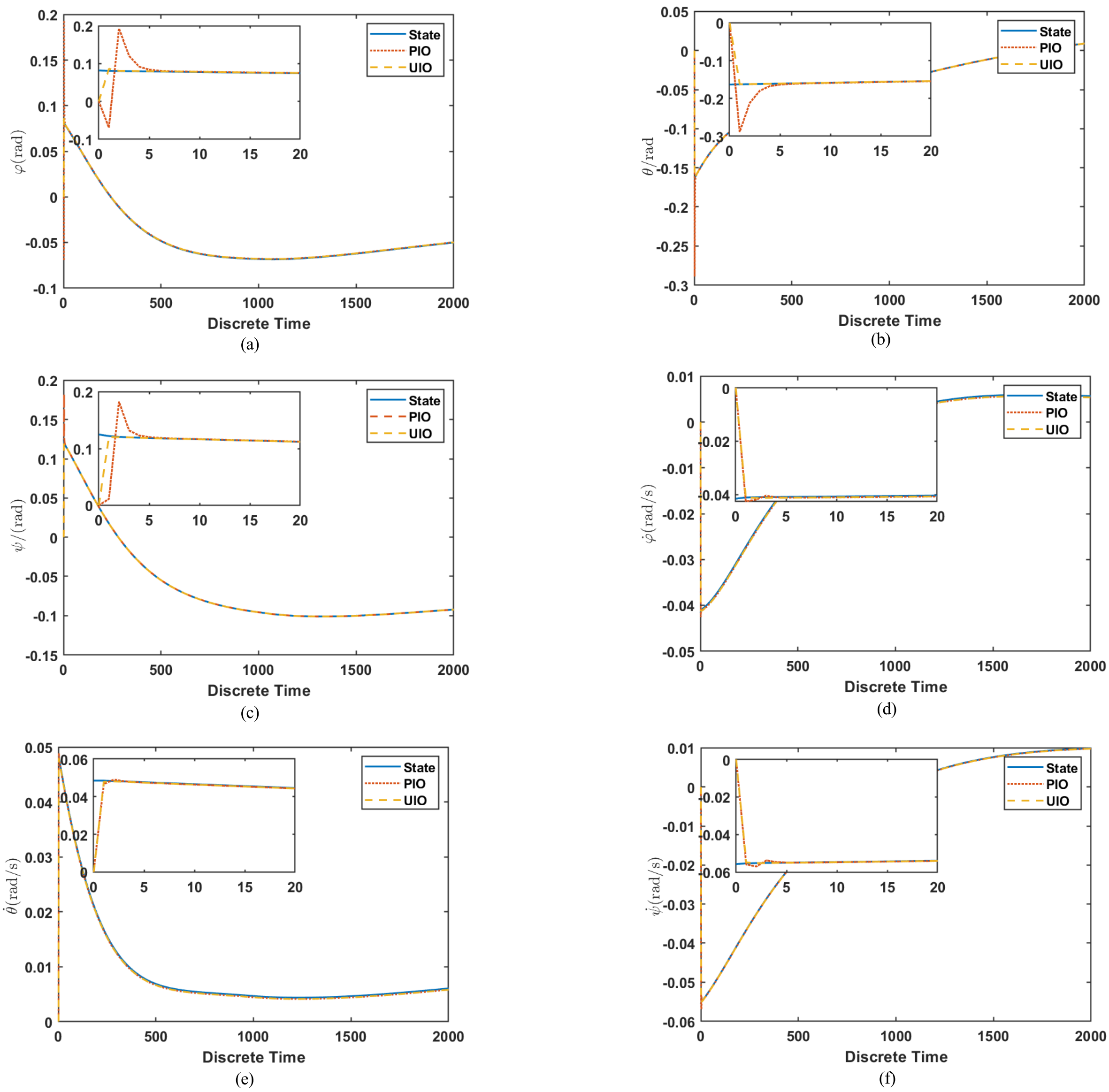

FIGURE 7. **Comparison of the real system state with state estimated by UIO and PIO. (a) Angle φ and its estimation; (b) Angle of θ and its estimation; (c) Angle of ψ and its estimation; (d) Angular velocity $\dot{\varphi}$ and its estimation; (e) Angular velocity $\dot{\theta}$ and its estimation; (f) Angular velocity $\dot{\psi}$ and its estimation.**

model. As it can be seen, the proposed neural state space model has an appropriate approximation property and can reflect the real system with relatively high accuracy.

Assume that actuator fault occurs in θ and ψ channels, and sensor fault occurs in φ channel. For the fault estimation purposes, we choose

$$f_s = \cos(kT_p) \tag{46}$$

and

$$f_a = \begin{cases} 0, & \text{if } k < 1000 \ (i.e.\ no\ actuator\ fault) \\ 0.005(kT_p - 10), & \text{if } 10000 \le k \ (i.e.\ actuator\ fault) \end{cases} \tag{47}$$

From the above known matrices, it can be calculated that the matrices $\boldsymbol{T}$ and $\boldsymbol{N}$ are respectively

$$\boldsymbol{T} = \begin{bmatrix} 1 & 0 & 0 & 0 & 0 & 0 \\ 0 & 1 & 0 & 0 & 0 & 0 \\ 0 & 0 & 1 & 0 & 0 & 0 \\ 0 & 0 & 0 & 1 & 0 & 0 \\ 0 & 0 & 0 & 0 & 1 & 0 \\ 0 & 0 & 0 & 0 & 0 & 1 \\ -1 & 0 & 0 & 0 & 0 & 0 \end{bmatrix}, \quad \boldsymbol{N} = \begin{bmatrix} 0 & 0 & 0 \\ 0 & 0 & 0 \\ 0 & 0 & 0 \\ 0 & 0 & 0 \\ 0 & 0 & 0 \\ 0 & 0 & 0 \\ 1 & 0 & 0 \end{bmatrix}.$$

According to the procedure of the UIO design for the actuator and sensor faults described above, the following values are obtained by solving the LMIs conditions (28), (29),

(30) using the LMI-toolbox in MATLAB

$$\mu = 0.4852, \quad \boldsymbol{k}_a = \begin{bmatrix} -0.0509 & -0.1212 & 0.1967 \\ 0.0110 & 0.0688 & -0.1039 \\ -0.055 & -0.3440 & 0.5196 \\ 0.0014 & 0.0252 & -0.0296 \\ 0.0001 & 0.0002 & -0.0011 \\ 0.0052 & 0.0278 & -0.0444 \\ 0.0509 & 0.1212 & -0.1967 \end{bmatrix}.$$

The initial conditions for the model (6) and the observer are:

$$\boldsymbol{x}(0) = [0.0847 \quad -0.1635 \quad 0.1248 \quad -0.0416 \quad 0.0484 \quad -0.0556 \quad 0.05]^T$$

and

$$\hat{\boldsymbol{x}}(0) = \begin{bmatrix} 0 & 0 & 0 & 0 & 0 & 0 & 0 \end{bmatrix}^T,$$

while the input is the ACS feedback control signal with $\boldsymbol{k}_p = 0.5\boldsymbol{I}_3, \boldsymbol{k}_d = 6\boldsymbol{I}_3$.

First, let us consider the case $\hat{\boldsymbol{x}}(0) = \boldsymbol{x}(0)$ when for $\boldsymbol{e}(0) = \boldsymbol{0}$. Fig. 5 clearly shows that $\Psi(k) < 0$ has always been negative, where $\Psi(k) = \Delta V(k) + \boldsymbol{e}_f^T(k)\boldsymbol{e}_f(k) - \mu^2\boldsymbol{\omega}^T(k)\boldsymbol{\omega}(k)$ so the condition (32) is satisfied. Then, it is assumed that $\boldsymbol{\omega}(k) = \boldsymbol{0}$ and $\hat{\boldsymbol{x}}(0) \neq \boldsymbol{x}(0)$. Fig. 6 clearly indicates that $\boldsymbol{e}(k) \to \boldsymbol{0}$ as k increases i.e. (31) is satisfied as well.

Fig. 7 shows the corresponding tracking performance for system's attitude angle and angular velocity respectively in case of $\boldsymbol{\omega}(k) \neq \boldsymbol{0}$ and $\hat{\boldsymbol{x}}(0) \neq \boldsymbol{x}(0)$. In order to show the performance of the proposed approach, the system state estimation results obtained by the traditional proportional

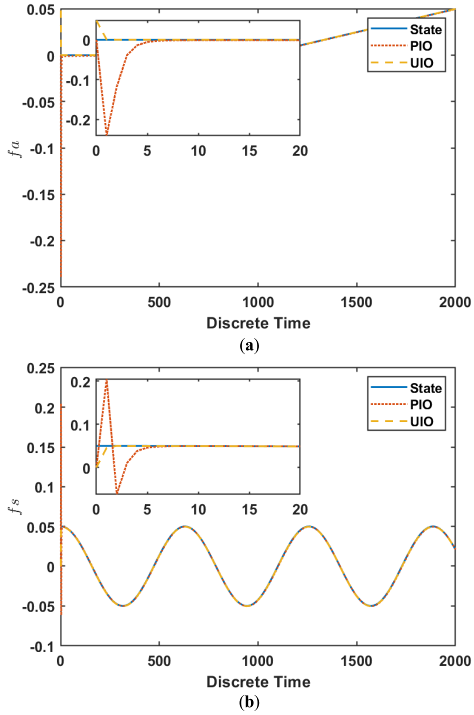

FIGURE 8. Comparison of the real system fault with fault estimated by UIO and PIO. (a) Actuator fault f_a and its estimation; (b) sensor fault f_s and its estimation.

$$\boldsymbol{A}^* = \begin{bmatrix} -0.1016 & -0.1211 & 0.1966 & -0.3097 & -0.7852 & -0.4013 \\ -0.0027 & -0.0036 & 0.0087 & -0.0003 & 0.0011 & 0.0074 \\ -0.1148 & -0.3585 & 0.5422 & 0.0342 & 0.0668 & -0.0304 \\ 0.0027 & 0.0252 & -0.0296 & 0.0041 & -0.0078 & -0.0036 \\ 0.0001 & 0.0002 & -0.0011 & -0.0018 & 0.0072 & -0.0008 \\ 0.0103 & 0.0278 & -0.0444 & 0.0035 & -0.0101 & 0.0020 \end{bmatrix},$$

$$\boldsymbol{B} = \begin{bmatrix} 1.1482 & -0.4831 & -0.9096 \\ 0.8168 & 0.3115 & -0.9415 \\ 1.1022 & -0.1673 & -0.7521 \\ -0.2629 & 0.0148 & 0.0790 \\ -0.0686 & -0.1907 & 0.0785 \\ -0.0908 & 0.0145 & -0.1047 \end{bmatrix},$$

$$\boldsymbol{A}_0 = \begin{bmatrix} -0.0265 & -0.0219 & -0.0271 & -0.0106 \\ 0.0003 & -0.0101 & -0.0097 & -0.0067 \\ -0.0254 & -0.0362 & -0.0374 & -0.0159 \\ -0.0012 & 0.0061 & 0.0005 & -0.0001 \\ -0.0019 & -0.0019 & -0.0012 & 0.0070 \\ -0.0056 & 0.0047 & 0.0049 & 0.0058 \end{bmatrix},$$

$$\boldsymbol{E}_0^* = \begin{bmatrix} 0.0023 & 0.0124 & 0.0114 & 0.0054 & 0.0024 & -0.0008 \\ 0.0138 & 0.0101 & -0.0118 & 0.0043 & 0.0057 & -0.0005 \\ 0.0052 & 0.0075 & -0.0052 & 0.0031 & -0.0013 & 0.0053 \\ 0.0136 & 0.0040 & -0.0070 & -0.0042 & -0.0089 & -0.0054 \end{bmatrix}.$$

integral observer (PIO) is also presented in Fig. 7. Note that the upper left of the figure brings up the zoomed part of the initial values.

In the same demonstration method. Fig. 8 presents the actuator and sensor fault values of satellite ACS and their estimated values via PIO and UIO. It is shown clearly in the figures, despite the presence of faults and disturbance, the proposed and traditional methods are both able to estimate the system state and different faults when two types of fault occur at the same time. However, the robust UIO shows the better performance than PIO. It has lower overshoot and faster convergence.

V. CONCLUSION

For the condition that the precise model of ACS cannot be obtained, a robust UIO design method based on RNN is proposed which can estimate the system state, actuator fault and sensor fault simultaneously. Firstly, the RNN is trained through system input and output to obtain weight matrices. With capability of generalization, the neural state space can be adaptive to the minor changes of real system. Then, we can expand the state vectors of the system to transform the neural state space model into a generalized nonlinear system without sensor fault term. Furthermore, a combination of the generalized observer scheme with the robust $H\infty$ LPV approach is developed to enhance the robustness of fault diagnosis. This method enables the observer to simul-taneously estimate state and actuator fault. Besides it can minimize the effect of exogenous disturbances. In the design process, the dynamic error is transformed into the discrete time polytopic LPV form, and the stability condition of the observer is analyzed by Lyapunov theory. Finally, the effectiveness of the proposed method is illustrated through simulations to solve the fault and state estimation for the ACS. The natural extension of the proposed approach is to design FTC strategy according to the obtained fault estimation results.

REFERENCES

[1] A. Rahimi, K. D. Kumar, and H. Alighanbari, "Fault isolation of reaction wheels for satellite attitude control," *IEEE Trans. Aerosp. Electron. Syst.*, vol. 56, no. 1, pp. 610–629, Feb. 2020.

[2] C. L. Li, X. Q. Chen, Q. X. Jia, and Y. H. Geng, "FDD of the attitude control system of satellite with actuator fault and time delay via two-stage Kalman filter," *Appl. Mech. Mater.*, vol. 441, pp. 859–863, Dec. 2013.

[3] T. Jiang, K. Khorasani, and S. Tafazoli, "Parameter estimation-based fault detection, isolation and recovery for nonlinear satellite models," *IEEE Trans. Control Syst. Technol.*, vol. 16, no. 4, pp. 799–808, Jul. 2008.

[4] Y. Yang, S. X. Ding, and L. Li, "Parameterization of nonlinear observer-based fault detection systems," *IEEE Trans. Autom. Control*, vol. 61, no. 11, pp. 3687–3692, Nov. 2016.

[5] L. Li, S. X. Ding, Y. Yang, K. Peng, and J. Qiu, "A fault detection approach for nonlinear systems based on data-driven realizations of fuzzy kernel representations," *IEEE Trans. Fuzzy Syst.*, vol. 26, no. 4, pp. 1800–1812, Aug. 2018.

[6] X. Wang, Z. Fei, H. Yan, and Y. Xu, "Dynamic event-triggered fault detection via zonotopic residual evaluation and its application to vehicle lateral dynamics," *IEEE Trans. Ind. Informat.*, vol. 16, no. 11, pp. 6952–6961, Nov. 2020.

[7] X. Wang, Z. Fei, H. Gao, and J. Yu, "Integral-based event-triggered fault detection filter design for unmanned surface vehicles," *IEEE Trans. Ind. Informat.*, vol. 15, no. 10, pp. 5626–5636, Oct. 2019.

[8] Z. Wang, P. Shi, and C.-C. Lim, "H_{-}/H_{∞} fault detection observer in finite frequency domain for linear parameter-varying descriptor systems," *Automatica*, vol. 86, pp. 38–45, Dec. 2017.

[9] H. Yang and H. Wang, "Robust adaptive fault-tolerant control for uncertain nonlinear system with unmodeled dynamics based on fuzzy approximation," *Neurocomputing*, vol. 173, pp. 1660–1670, Jan. 2016.

[10] S. Yin, B. Xiao, S. X. Ding, and D. Zhou, "A review on recent development of spacecraft attitude fault tolerant control system," *IEEE Trans. Ind. Electron.*, vol. 63, no. 5, pp. 3311–3320, May 2016.

[11] M. M. Tavakoli and N. Assadian, "Predictive fault-tolerant control of an all-thruster satellite in 6-DOF motion via neural network model updating," *Adv. Space Res.*, vol. 61, no. 6, pp. 1588–1599, Mar. 2018.

[12] Z. Fei, X. Wang, M. Liu, and J. Yu, "Reliable control for vehicle active suspension systems under event-triggered scheme with frequency range limitation," *IEEE Trans. Syst., Man, Cybern. Syst.*, early access, Mar. 12, 2019, doi: 10.1109/TSMC.2019.2899942.

[13] Y. Shen, Z. Wang, and X. Zhang, "Fault diagnosis and fault-tolerant control for sampled-data attitude control systems: An indirect approach," *Proc. Inst. Mech. Eng., G, J. Aerosp. Eng.*, vol. 228, no. 7, pp. 1047–1057, Jun. 2014.

[14] Q. Jia, W. Chen, Y. Zhang, and H. Li, "Integrated design of fault reconstruction and fault-tolerant control against actuator faults using learning observers," *Int. J. Syst. Sci.*, vol. 47, no. 16, pp. 3749–3761, Dec. 2016.

[15] Y. Cheng, R. Wang, M. Xu, and Y. Li, "Simultaneous state and actuator fault estimation for satellite attitude control systems," *Chin. J. Aeronaut.*, vol. 29, no. 3, pp. 714–721, Jun. 2016.

[16] E. Naderi and K. Khorasani, "A data-driven approach to actuator and sensor fault detection, isolation and estimation in discrete-time linear systems," *Automatica*, vol. 85, pp. 165–178, Nov. 2017.

[17] C. Gao, Q. Zhao, and G. Duan, "Robust actuator fault diagnosis scheme for satellite attitude control systems," *J. Franklin Inst.*, vol. 350, no. 9, pp. 2560–2580, Nov. 2013.

[18] J. Zhang, A. K. Swain, and S. K. Nguang, "Robust sensor fault estimation scheme for satellite attitude control systems," *J. Franklin Inst.*, vol. 350, no. 9, pp. 2581–2604, Nov. 2013.

[19] A. Zhang, Q. Hu, and Y. Zhang, "Observer-based attitude control for satellite under actuator fault," *J. Guid., Control, Dyn.*, vol. 38, no. 4, pp. 806–811, Apr. 2015.

[20] M. Defoort, K. C. Veluvolu, J. J. Rath, and M. Djemai, "Adaptive sensor and actuator fault estimation for a class of uncertain Lipschitz nonlinear systems," *Int. J. Adapt. Control Signal Process.*, vol. 30, no. 2, pp. 271–283, Feb. 2016.

[21] D. Ichalal, B. Marx, J. Ragot, and D. Maquin, "Unknown input observer for LPV systems with parameter varying output equation," in *Proc. 9th IFAC Symp. Fault Detection, Supervision Saf. Tech. Processes (Safeprocess)*, 2015, pp. 1030–1035.

[22] J. Na, A. S. Chen, G. Herrmann, R. Burke, and C. Brace, "Vehicle engine torque estimation via unknown input observer and adaptive parameter estimation," *IEEE Trans. Veh. Technol.*, vol. 67, no. 1, pp. 409–422, Jan. 2018.

[23] M. Mrugalski, M. Luzar, M. Pazera, M. Witczak, and C. Aubrun, "Neural network-based robust actuator fault diagnosis for a non-linear multi-tank system," *ISA Trans.*, vol. 61, pp. 318–328, Mar. 2016.

[24] G. Wen, C. L. P. Chen, Y. J. Liu, and Z. Liu, "Neural network-based adaptive leader-following consensus control for a class of nonlinear multiagent state-delay systems," *IEEE Trans. Cybern.*, vol. 47, no. 8, pp. 2151–2160, Aug. 2017.

[25] P. Witczak, K. Patan, M. Witczak, and M. Mrugalski, "A neural network approach to simultaneous state and actuator fault estimation under unknown input decoupling," *Neurocomputing*, vol. 250, pp. 65–75, Aug. 2017.

[26] Z. Zhang, Y. Lu, L. Zheng, S. Li, Z. Yu, and Y. Li, "A new varying-parameter convergent-differential neural-network for solving time-varying convex QP problem constrained by linear-equality," *IEEE Trans. Autom. Control*, vol. 63, no. 12, pp. 4110–4125, Dec. 2018.

[27] W.-K. Tam and Z. Yang, "Neural parallel engine: A toolbox for massively parallel neural signal processing," *J. Neurosci. Methods*, vol. 301, pp. 18–33, May 2018.

[28] H. Abbas and H. Werner, "Polytopic quasi-LPV models based on neural state-space models and application to air charge control of a Si engine," *IFAC Proc. Volumes*, vol. 41, no. 2, pp. 6466–6471, 2008.

[29] M. Mrugalski, "An unscented Kalman filter in designing dynamic GMDH neural networks for robust fault detection," *Int. J. Appl. Math. Comput. Sci.*, vol. 23, no. 1, pp. 157–169, Mar. 2013.

[30] P. Gil, J. Henriques, A. Dourado, and H. Duarte-Ramos, "On state-space neural networks for systems identification: Stability and complexity," in *Proc. IEEE Conf. Cybern. Intell. Syst.*, Jun. 2006, pp. 1–5.

[31] N. Hirose and R. Tajima, "Modeling of rolling friction by recurrent neural network using LSTM," in *Proc. IEEE Int. Conf. Robot. Autom. (ICRA)*, May 2017, pp. 6471–6478.

[32] Z. Sun, Y. Cheng, and Y. Geng, "The active magnetic control algorithm for HITSAT-1," *Aircr. Eng. Aerosp. Technol. Int. J.*, vol. 72, no. 2, pp. 137–141, 2000.

[33] Q. Jia, W. Chen, Y. Zhang, and H. Li, "Fault reconstruction for continuous-time systems via learning observers," *Asian J. Control*, vol. 18, no. 2, pp. 549–561, Mar. 2016.

[34] Z. G. Han, "Fault reconstruction and tolerant control technology for spacecraft attitude control systems," Ph.D. dissertation, Dept. Elect. Eng., NPU Univ., Xi'an, China, 2017.

DIZHI LONG received the B.S. degree from the College of Aerospace, Nanjing University of Aeronautics and Astronautics, Nanjing, China, in 2017, where he is currently pursuing the Ph.D. degree. His research interests include neural network-based fault diagnosis, spacecraft control, and state estimation theory.

XIN WEN was born in 1961. He received the M.S. and Ph.D. degrees in control engineering from the Harbin Institute of Technology, Harbin, China, in 1993 and 1995, respectively. He is currently a Professor with the College of Aerospace, Nanjing University of Aeronautics and Astronautics. His major research interests include formation control of satellites, fault detection, and intelligent control.

WEI ZHANG received the M.S. degree in electronics and communication engineering from Chonnam National University, South Korea. He is currently an Associate Professor with the College of Information Engineering, Beijing Institute of Petrochemical Technology. His major research interests include signal processing, satellite navigation, aerospace information engineering, and fault diagnosis.

JUNHONG WANG received the B.S. degree from the College of Mechatronics Engineering, North University of China, Shanxi, China, in 2018. He is currently pursuing the M.E. degree with the College of Aerospace, Nanjing University of Aeronautics and Astronautics, Nanjing, China. His research interests include neural network-based fault diagnosis, rocket control, and state estimation theory.